1854 *Biochemistry* **2010,** *49,* 1854–1861
DOI: 10.1021/bi901850n

BIOCHEMISTRY
including biophysical chemistry & molecular biology
Article

Assessing the Role of Oxidized Methionine at Position 213 in the Formation of Prions in Hamsters[†]

Christopher J. Silva,*[,‡] Bruce C. Onisko,[§] Irina Dynin,[‡] Melissa L. Erickson,[‡] William H. Vensel,[‡] Jesús R. Requena,[∥] Elizabeth M. Antaki,[‡,⊥] and John Mark Carter[‡]

[‡]*Western Regional Research Center, United States Department of Agriculture, Albany, California 94710,* [§]*OniPro Biosciences, Kensington, California 94707, and* [∥]*Prion Research Unit, Department of Medicine, School of Medicine, University of Santiago, Santiago, Spain* [⊥]*Present address: University of California, Davis, CA 95616.*

Received October 28, 2009; Revised Manuscript Received January 31, 2010

ABSTRACT: Prions are infectious proteins that are able to recruit a normal cellular prion protein and convert it into a prion. The mechanism of this conversion is unknown. Detailed analysis of the normal cellular prion protein and a corresponding prion has shown they possess identical post-translational modifications and differ solely in conformation. Recent work has suggested that the oxidized form of the methionine at position 213 (Met213) plays a role in the conversion of the normal cellular prion protein to the prion conformation and is a prion-specific covalent signature. We developed a sensitive method of quantitating the methionine sulfoxide present at position 213 (MetSO213) and used this method to measure the changes in MetSO213 over the time course of an intracranial challenge, using the 263K strain of hamster-adapted scrapie. These results indicate that the proportion of Met213 that is oxidized decreases over the course of the disease. We examined the quantity of MetSO213 in PrP^C and compared it to the amount found in animals terminally afflicted with the 263K, 139H, and drowsy strains of hamster-adapted scrapie. These strains show only low levels of MetSO213 that is comparable to that of PrP^C. These data suggest that MetSO213 does not appear to be a prion-specific covalent signature.

Transmissible spongiform encephalopathies (TSEs)[1] make up a set of rare fatal neurological diseases caused by a novel pathogen, a prion. Prions are able to recruit the normal cellular prion protein (PrP^C) and convert it into a prion (PrP^{Sc}) and thereby propagate an infection (*1*, *2*). TSEs are known to afflict agriculturally important animals such as sheep and cows (*3*, *4*). In addition, wild and captive deer, elk, moose, mink, and zoo animals are susceptible to TSEs (*5*−*7*). In humans, prion diseases are known as Creutzfeldt-Jakob disease (CJD), Gerstmann-Sträussler-Scheinker disease, kuru, or fatal familial insomnia. They can be inherited, sporadic, or transmitted. TSEs are characterized by an extended asymptomatic incubation period followed by a relatively short disease course ending in death. During the course of the disease, there is no immune response.

Detailed analysis of the structures of PrP^C and PrP^{Sc} has shown that PrP^C and PrP^{Sc} have identical amino acid sequences, a single disulfide bond, covalently attached sugar antennae, and a single glycophosphatidylinositol (GPI) anchor (*8*, *9*). The primary amino acid sequences of PrP^C and PrP^{Sc} are identical. Other than those already enumerated, no post-translational modifications of the amino acids have been identified in PrP^{Sc}. The sugar antennae are covalently bound to asparagine residues at positions 181 and 197 (in hamsters) (*8*−*10*). The composition of the sugar antennae is variable but varies similarly in both PrP^C and PrP^{Sc} (*10*, *11*). The variation in the sugar composition of the GPI anchor is similar in both PrP^C and PrP^{Sc} (*12*). These experiments show that there is no covalent difference between PrP^C and PrP^{Sc}.

Since there are no covalent differences between PrP^C and PrP^{Sc}, they must differ in their respective conformations. Circular dichroism and infrared spectroscopy have been used to establish that the secondary structure of PrP^{Sc} is comprised of a high proportion of β-sheet structure (*13*, *14*). NMR studies of PrP^C show that it is composed of an amino-terminal unstructured domain and α-helices (*15*, *16*). There is very little β-sheet present in PrP^C. This conversion from the unordered and α-helical secondary structure of PrP^C to the β-sheet secondary structure of PrP^{Sc} is responsible for the properties of prions.

Oxidation of methionine has been associated with conformational differences in model systems (*17*). The structure of recombinant hamster PrP with oxidized methionines is very similar to that of recombinant hamster PrP without oxidized methionines, as measured by circular dichroism (*18*). Other researchers have observed that the ability of recombinant hamster PrP to form fibrils is dependent upon the level of methionine oxidation (*19*). The role of specific oxidized methionines has been studied in model systems. One study used a portion of the human PrP protein (amino acid residues 125−229) and molecular modeling (*20*). In another study, the methionines in full-length recombinant hamster PrP were selectively replaced with the synthetic methionine analogue norleucine or methoxinine (*21*).

[†]This work was supported in part by Grant BFU2006-04588/BMC from the Spanish Ministry of Science and Education and Grant FOOD-CT-2006-023183 from the European Union to J.R.R.

*To whom correspondence should be addressed: USDA, ARS, 800 Buchanan St., Albany, CA 94706. E-mail: christopher.silva@ars.usda.gov. Telephone: (510) 559-6136. Fax: (510) 559-5758.

[1]Abbreviations: Met213, methionine at amino acid position 213; MetSO213, methionine sulfoxide at amino acid position 213; TSE, transmissible spongiform encephalopathy; CJD, Creutzfeldt-Jakbob disease; GPI, glycophosphatidylinositol; SDS−PAGE, sodium dodecyl sulfate−polyacrylamide gel electrophoresis; BOG, β-octyl glucopyranoside; DTT, dithiothreitol; CV, coefficient of variation; MRM, multiple-reaction monitoring; MetSO, methionine sulfoxide; PK, proteinase K.

 Published on Web 02/02/2010

Both of these studies showed that oxidation of the methionine at position 213 facilitated a conformational conversion of the region containing that methionine from α-helix to β-sheet secondary structure. Such a transformation may be important in the origin of PrP^{Sc}.

Recent experimental work has concluded the oxidation of Met213 is a covalent signature of PrP^{Sc} (*22*). These results are surprising since Met213 is not as accessible as the other methionines present in the molecule and, as a result, is more resistant to peroxide oxidation (*18*). Methionine oxidation can occur during the general handling of proteins (*23*−*25*), during SDS−PAGE (*26*, *27*), and even during the electrospray ionization process (*28*, *29*). Stahl et al. noticed the occasional presence of oxidized methionines at position 206 and/or position 213 during their mass spectrometric analysis of the structure of PrP^{Sc} (*9*). The origin of these modifications was unclear, and Stahl et al. concluded that PrP^{C} and PrP^{Sc} possess no covalent differences. It is, therefore, important to employ an analytical method that does not facilitate the oxidation of methionine (*26*).

We developed a mass spectrometry-based assay for the detection of a peptide fragment containing residues 209−220 from the normal cellular prion protein or prions in brains of infected laboratory hamsters (*30*, *31*). We used nanoscale chromatography with tandem mass spectrometry to detect and quantitate the amount of this peptide and the corresponding sulfoxide present in the brains of healthy and prion-infected animals. We report these results here.

EXPERIMENTAL PROCEDURES

Chemicals. Trypsin (porcine, sequencing grade, modified) was purchased from Promega (Madison, WI). The iodoacetamide derivatives of the peptide VVEQMCTTQYQK, the corresponding sulfoxide, and the isotopically enriched peptide (internal standard) were synthesized by Anaspec (Fremont, CA). The sulfoxide and the peptide differed solely in terms of the presence of the oxygen on the sulfur of methionine. The peptide and the internal standard differed in terms of the isotope content of the terminal valine, either natural isotopic abundance or [$^{13}C_5$,^{15}N]valine. The peptide and the sulfoxide-containing peptide had different chromatographic mobilities. The chromatographic mobilities of the internal standard and peptide were identical. The composition of these synthetic peptides was confirmed by mass spectrometry. The chemical purity was greater than 90% as shown by LC/UV, and the isotopic purity was greater than 99.8%. The structure of each peptide was verified by amino acid analysis and mass spectrometry (Anaspec). HPLC grade water was purchased from Burdick and Jackson (Muskegon, MI). Acetonitrile (HPLC grade) was from Fisher Scientific (Fairlawn, NJ). All other reagents were from Sigma-Aldrich (St. Louis, MO).

Syrian Hamster PrP Animal Handling and Sample Preparation. The 263K strain of hamster-adapted scrapie (*32*, *33*) and the drowsy strain of hamster-adapted mink encephalopathy (*34*) were obtained from InPro Biotechnology (South San Francisco, CA) and passaged once through LVG Syrian golden hamsters (Charles River Laboratories, Wilmington, MA). The 139H strain of hamster-adapted scrapie (*35*) was a gift from R. I. Carp, and it was passaged once through LVG Syrian golden hamsters. Forty female LVG hamsters (4 weeks old) were inoculated intracranially (*ic*) with 50 μL of a 1% brain homogenate, prepared from a terminal-stage animal. Four hamsters were anesthetized with isoflurane and euthanized by cervical dislocation starting 1 week after inoculation and then continuing weekly for 10 weeks, when the animals displayed symptoms. The spinal column was severed from the base of the skull with surgical scissors. Each brain was quickly removed from the skull and immediately frozen at −80 °C. The surgical equipment was wiped with 1 M sodium hydroxide and then 70% ethanol between each brain removal. After the four brains were removed, the surgical equipment was cleaned as described and then soaked in a phenolic solution to remove any prions and minimize any cross contamination (*36*).

Each brain was homogenized and centrifuged in disposable plasticware. Only a single group of four brains was processed on the same day, to minimize any chance of cross contamination. Using the method of Diringer et al. (*37*), the P145a pellet was obtained from a 20% aliquot of each brain homogenate. Each brain was homogenized in 12.5 mL of homogenization buffer [10% solution of *N*-lauroylsarcosine, 9.5 mM sodium phosphate (pH 8.5), and protease inhibitors]. After 30 min at room temperature, the homogenate was centrifuged for 18 min at 16000*g* in a Beckman 70.1 Ti rotor. The supernatant was collected, and 20% of the total supernatant volume was combined with 1 mL of 0.1 M EDTA (pH 7.6). The volume was increased to 12 mL with homogenization buffer and underlain with 1 mL of 20% sucrose in water. The sample was centrifuged at 145000*g* in a Beckman 70.1 Ti rotor to obtain an insoluble pellet, P145a, which was then treated with proteinase K for 1 h at 37 °C. The proteinase K was inactivated by the addition of 1% (v/v) proteinase inhibitor cocktail (Sigma). The resulting PrP 27−30 was denatured by addition of a sufficient amount of 8 M guanidine hydrochloride to achieve a final concentration of 6 M (*38*). The 6 M guanidine solution containing the denatured PrP 27−30 was allowed to stand for at least 24 h before precipitation. Protein was precipitated by addition of 5 volumes of methanol at −20 °C, and the mixture was centrifuged at 20000*g* for 20 min with an Eppendorf (Hamburg, Germany) model 5417R centrifuge.

Purification of PrP^{C} from the Brains of Uninfected Hamsters. The brains from 300 healthy uninfected hamsters were surgically removed from animals that were previously anesthetized with isoflurane and euthanized by cervical dislocation. After removal, the brains were immediately frozen on dry ice and then stored in a −80 °C freezer until needed. The brains were homogenized in a steel blender with liquid nitrogen until they were pulverized into a fine powder. The powder was stored in a −80 °C freezer until needed. The synaptosomal/microsomal membranes were isolated by the method of Pergami et al. (*39*). Forty grams of the brain powder was homogenized in 200 mL of buffer (0.32 M sucrose, 0.5 mM KCl, 1 mM $MgCl_2$, 1 mM $NaHCO_3$, 1 mM dithiothreitol, and 5 mM phenylmethanesulfonyl fluoride). The homogenate was centrifuged at 3000*g* and 4 °C for 10 min. The supernatant was removed. The pellet was rehomogenized using the same buffer and centrifuged under the same conditions. This second supernatant was removed and combined with the other supernatant. The combined supernatants were divided among eight ultracentrifuge tubes subjected to ultracentrifugation (Beckman 70 Ti rotor) at 100000*g* for 1 h at 4 °C over a 0.85 M sucrose cushion. The resulting supernatant was removed, and one of the pellets was dissolved, by being gently stirred at room temperature for 30 min in 28 mL of buffer [25 mM phosphate (pH 7.4) with 2% (w/v) β-octyl glucopyranoside]. The solution from the redissolved pellet was subjected to

ultracentrifugation (Beckman 70.1 Ti rotor) at 100000*g* for 1 h at 15 °C. The supernatant from this ultracentrifugation was retained and the pellet discarded.

The supernatant was subjected to cation exchange chromatography. It was loaded onto a Vivapure Maxi spin column (Vivascience Stonehouse) that had been prepared and washed according to the manufacturer's instructions. It was spun at 500*g* for 5 min. The flow-through was discarded. The column was loaded with 5 mL of buffer [25 mM phosphate (pH 7.4) with 1% (w/v) β-octyl glucopyranoside] and spun at 500*g* for 5 min. The wash was discarded. The washing continued in 5 mL steps with 50, 100, and 200 mM NaCl buffers [25 mM phosphate (pH 7.4) with 1% (w/v) β-octyl glucopyranoside]. The final elution with 500 mM NaCl was retained and subjected to immobilized metal affinity chromatography.

The 1 mL HIS-Select cartridge (Sigma Corp., Milwaukee, WI) was stripped and recharged with copper according to the manufacturer's instructions. The final elution from the cation exchange column was added to the cartridge at a flow rate of 1 mL/min. After the cartridge was loaded, it was washed once with 5 mL of buffer [500 mM NaCl, 25 mM phosphate (pH 7.4), and 1% (w/v) β-octyl glucopyranoside] and twice with 5 mL of buffer [50 mM NaCl, 25 mM phosphate (pH 7.4), and 1% (w/v) β-octyl glucopyranoside]. The washes were discarded. The cartridge was eluted sequentially with 5 mL of buffer [50 mM NaCl, 25 mM phosphate (pH 7.4), and 1% (w/v) β-octyl glucopyranoside] containing 10 mM, 50 mM, and finally 100 mM imidazole. The 5 mL fraction eluted with 50 mM imidazole was concentrated with an Amicon Ultra centrifugal filter device (10K cutoff; Millipore Corp., Billerica, MA) and then precipitated with methanol. The pellet was redissolved and subjected to analysis by mass spectrometry (vide infra).

Reduction, Alkylation, and Tryptic Cleavage of Syrian Hamster PrP Samples. The whole pellet obtained after methanol precipitation (vide supra) was sonicated for 5 min in a 10 μL solution of 0.01% aqueous β-octyl glucopyranoside (BOG). After sonication, a 10 μL solution containing the internal standard ([$^{13}C_5$,^{15}N]VVEQMCTTQYQK, 18 fmol/μL in 0.01% aqueous BOG) was added and the mixture sonicated for an additional 5 min. Ten microliters of a solution of 10 mM dithiothreitol (DTT) in buffer A (25 mM ammonium bicarbonate, 0.01% BOG, and 1 pmol/μL methionine) was added to the mixture and the mixture allowed to react for 1 h at 37 °C and then cooled to room temperature. Forty microliters of a solution of buffer A containing 10 mM iodoacetamide was added to the mixture and allowed to stand in the dark at room temperature for 1 h. The excess iodoacetamide was quenched by addition of 20 μL of a solution containing 10 mM DTT in buffer A. The reduced and alkylated peptides were subjected to proteolysis by the addition of 10 μL of a trypsin solution (100 μg of trypsin/mL of water). The reaction was allowed to proceed at 37 °C for 16 h. Samples were stored at −20 °C until they were analyzed.

Reduction, Alkylation, and Tryptic Cleavage of the Sulfoxide of the VVEQMCTTQYQK Peptide. Twelve identical 20 μL solutions of 0.01% BOG containing 1 pmol of the synthetic sulfoxide peptide and 180 fmol of the isotopically labeled peptide were prepared. Four were diluted with 0.01% BOG to yield a final volume of 100 μL. These four were analyzed by mass spectrometry (vide infra). Ten microliters of a solution of 10 mM dithiothreitol (DTT) in buffer A was added to each of the remaining eight samples and the mixture allowed to react for 1 h at 37 °C and then cooled to room temperature. Forty microliters of a solution of buffer A containing 10 mM iodoacetamide was added to each of these eight samples and the mixture allowed to stand for 1 h at room temperature in the dark. The excess iodoacetamide present in the eight samples was quenched by addition of 20 μL of a solution containing 10 mM DTT in buffer A. Ten microliters of 0.01% BOG was added to four of the eight samples. These four were subjected to analysis by mass spectrometry (vide infra). The four remaining samples were subjected to proteolysis by the addition of 10 μL of a trypsin solution (100 μg of trypsin/mL of water). The reaction was allowed to proceed at 37 °C for 16 h. These last four samples were analyzed by mass spectrometry (vide infra).

Quantitative Mass Spectrometry: Nanospray LC−MS/MS. An Applied Biosystems (ABI/MDS Sciex, Toronto, ON) model 4000 Q-Trap instrument equipped with a nanoelectrospray source was used to perform nanospray liquid chromatography and tandem mass spectroscopy (LC−MS/MS). An aliquot (6 μL) of each digest (10.8 fmol of internal standard) was loaded onto a C-18 trap cartridge [PepMap, 5 μm, 100A, 300 μm (inside diameter) × 5 mm (Dionex, Sunnyvale, CA)]. Salts were washed from the cartridge with an acetic acid/acetonitrile/heptafluorobutyric acid/water solution (0.5/1/0.02/99). The now salt-free bound peptides were eluted onto a reversed-phase column [Vydac (Hesperia, CA) 238EV5.07515, 75 μm × 150 mm].

The solvents were delivered with an Applied Biosystems model Tempo nanoflow LC system (ABI/MDS Sciex) with an autosampler, a column switching device, and a nanoflow solvent delivery system. Samples were eluted from the column with a binary gradient (A, 0.5% acetic acid in water, and B, 80% acetonitrile with 0.5% acetic acid). The flow rate was 250 nL/min with a 16 min linear gradient starting with 5% B and ending with 100% B. Elution with 100% B was conducted for 7 min followed by a return to 5% B over 4 min. The eluted samples were sprayed with a noncoated spray tip (FS360-20-10-N-20-C12, New Objective Inc., Woburn, MA) onto the Applied Biosystems source, Model Nanospray II.

The mass spectrometer was operated in multiple-reaction monitoring (MRM) mode, alternating among detection of VVEQMCTTQYQK (precursor ion at *m*/*z* 757.8, product ion at *m*/*z* 171.1), the sulfoxide (precursor ion at *m*/*z* 765.8, product ion at *m*/*z* 171.1), and [$^{13}C_5$,^{15}N]VVEQMCTTQYQK (precursor ion at *m*/*z* 760.8, product ion at *m*/*z* 177.1). Both quadrupoles were operated at unit resolution (full width at half-maximum of 0.7 Da). Fragmentation to obtain the specified product ion was optimized via adjustment of the Q2 offset voltage (collision "energy") to a value of 45 V for all three ion reactions. Quantitation was conducted with the Intelliquan quantitation algorithm using Analyst version 1.4.1.

RESULTS

A series of solutions containing known but varying concentrations of the analyte peptide [residues 209−220 (VVEQMCTTQYQK)] or the sulfoxide of the analyte peptide and a fixed amount of the isotopically labeled internal standard were prepared. These solutions were analyzed with the triple quadrupole mass spectrometer. The area ratio of the integrated signal from the analyte peptide or the sulfoxide of the analyte peptide to that of the isotopic standard was used to prepare a calibration curve. The calibration curves for the analyte peptide (A) and the sulfoxide of the analyte peptide (B) are shown in Figure 1. The correlation coefficient for both of these linear curves is 0.99. Furthermore,

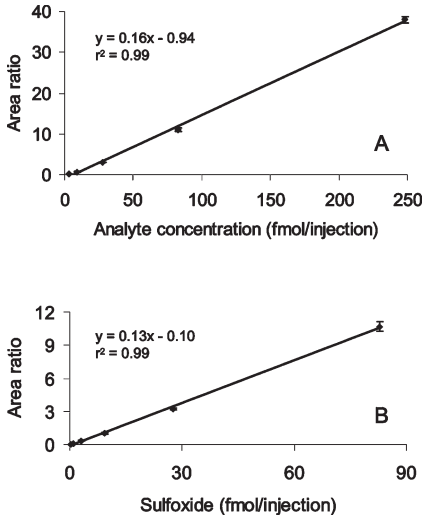

FIGURE 1: Calibration curves used to determine the empirical relationship between the concentration of the analyte peptide (A) and analyte methionine sulfoxide (B) and the ^{13}C-labeled internal standard. All concentrations are reported as the mean ± standard deviation of four injections.

the coefficient of variation (CV) for these area ratios is small, ranging from 0.9 to 3.8%. The CV for the analyte retention time was small, averaging 2.0%. The results indicate that this method provides an accurate and reproducible way of quantitating the analyte peptide, its corresponding sulfoxide, and the ratio of the two.

The isotopically labeled internal standard and the analyte peptide (VVEQMCTTQYQK) have identical chemical properties, except for a mass difference of 6 Da. While the differences in molecular mass are easily detected by mass spectrometry, they do not significantly change the retention times of these molecules. This allows the use of the internal standard to confirm the identity of the analyte peptide by its characteristic chromatographic retention time and by its characteristic molecular mass. It also allows us to mark the presence of the sulfoxide of the analyte peptide, based on its relative chromatographic retention time and its characteristic molecular mass.

To quantitate the analyte peptide or the oxidized form of the analyte peptide, we operate our mass spectrometer in the MRM mode. We set our instrument to isolate ions with a mass-to-charge ratio corresponding to our analyte peptide (m/z 757.8; $z = 2$), the oxidized analyte peptide (m/z 765.8; $z = 2$), the isotopically labeled internal standard (m/z 760.8; $z = 2$), and the oxidized isotopically labeled internal standard (m/z 768.8; $z = 2$). Only ions with these predefined mass-to-charge ratios are sequentially permitted into the collision cell. After an ion with one of these four predefined mass-to-charge ratios enters the collision cell, it is fragmented by collision with nitrogen gas. The ions from this collision are analyzed, and the intensity of the signal from a distinct fragment [a_2 ion of the peptide; m/z 171.1 (analyte) or m/z 177.1 (internal standard)] is recorded.

We were concerned that other molecules might produce signals that would interfere with our quantitation method. For such interference to occur, a molecule would need to possess a chromatographic retention time similar to that of the analyte peptide and generate a fragment with a m/z of 171.1. A combination of these diverse properties is highly unlikely, but not impossible. To test this, we removed the brains from three uninfected control hamsters. Each of these brains was homogenized and subjected to the PrP 27−30 isolation procedure. The resulting pellet was subjected to mass spectrometric analysis using the internal standards. These results, shown in Figure 2, demonstrate that healthy control animals possess no molecule with an observable signal having a retention time corresponding to that of the isotopically labeled internal standard (Figure 2, graph 1) or the oxidized isotopically labeled internal standard (Figure 2, graph 2). We conclude, therefore, that there are no interfering molecules present in a healthy hamster brain and that the signals we observe from infected brains result from PrP 27−30.

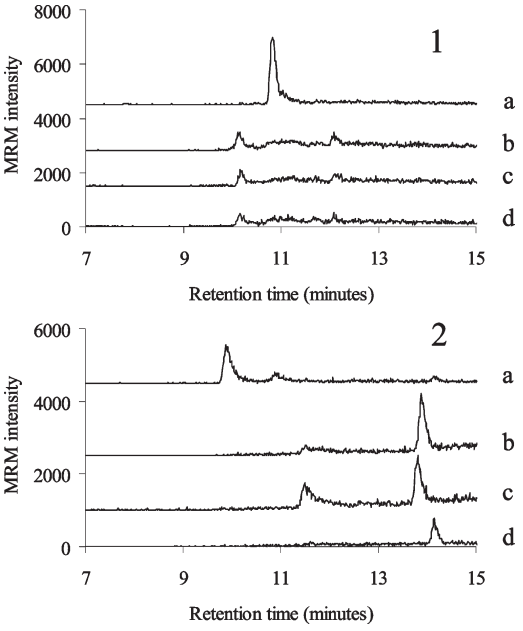

FIGURE 2: Determining the background interference from non-PrP 27−30 molecules. Chromatograms a−d are offset for the sake of clarity. Chromatogram a is from an isotopically labeled internal standard. Chromatograms b−d are from brains of healthy control animals subjected to the PrP 27−30 isolation procedure and mass spectrometric analysis. Graph 1 shows four multiple-reaction monitoring (MRM) chromatograms using a mass window that is selective for either the unoxidized isotopically labeled internal standard (a) or the unoxidized analyte peptide (b−d). Graph 2 shows four MRM chromatograms using a mass window that is selective for either the oxidized isotopically labeled internal standard (a) or the oxidized analyte peptide (b−d).

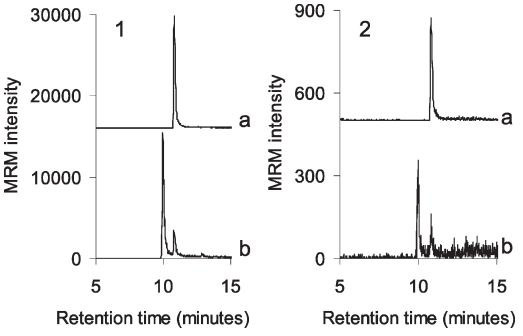

FIGURE 3: Assessing the electrospray-induced oxidation of the analyte peptide. Multiple-reaction monitoring (MRM) chromatogram (chromatograms are offset for the sake of clarity) using a mass window that is selective for either the unoxidized peptide (intensity × $^1/_{10}$) (a) or the oxidized peptide (b). Graph 1 shows the result from a PK-treated brain from a symptomatic animal infected with the 263K strain of hamster-adapted scrapie. Graph 2 shows the results with the $^{13}C_5$- and ^{15}N-labeled synthetic peptide used as an internal standard.

Figure 3 shows chromatograms for the analyte peptide isolated from the brain of a symptomatic hamster infected with the 263K

strain of hamster-adapted scrapie and the chromatogram of the isotopically labeled internal standard. The top traces record the intensity of the MRM signal from the unoxidized methionine of the analyte peptide or the labeled internal standard. The bottom traces record the MRM signal intensity from the methionine sulfoxide form of the analyte peptide or the labeled internal standard. These traces show that the sulfoxide form of the peptide (the sulfoxide diastereoisomers coelute) and the peptide have a baseline separation with no tailing. This indicates there is no aggregation of these peptides, which has been seen previously with peptides resulting from LysC cleavage (*9*). The peak with a retention time of 10.85 min (1a and 2a) corresponds to the unoxidized peptide. The peak with a retention time of 9.98 min (1b and 2b) corresponds to the oxidized peptide. The small peak in traces 1b and 2b with a retention time of 10.85 min corresponds to the fraction of the unoxidized peptide (a) that is oxidized during the electrospray ionization (*28*, *29*). If the peptide was oxidized before it was chromatographed, then it would have a different retention time. A similar result can be seen in Figure 2 (graph 2, chromatogram a). From this, we conclude that under our electrospray conditions, there is little electrospray-induced oxidation of methionine ($2 \pm 0.3\%$).

We were concerned that the reduction and alkylation necessary for mass spectrometry might also reduce a significant amount of MetSO213 to Met213 (*40*). To test this hypothesis, we performed the reduction, alkylation, and trypsin cleavage necessary for our mass spectrometric analysis on 1 pmol of the sulfoxide of the synthetic peptide. We prepared three sets (four replicates per set) of aliquots of this sulfoxide. One set was analyzed by mass spectrometry without reduction and alkylation or trypsin cleavage. The second set was subjected to the reduction and alkylation procedure, but not the trypsin cleavage, and then analyzed by mass spectrometry. The third set was subjected to all three and then analyzed by mass spectrometry.

The area ratio of the reduced peptide to the starting sulfoxide was determined for each quadruplicate set. In the first set, the ratio was 0.0004 ± 0.0004. After alkylation and reduction, the ratio was 0.0006 ± 0.0001. The quadruplicate set subjected to reduction, alkylation, and trypsin cleavage had a ratio of 0.001 ± 0.0002. This indicates that approximately 0.1% of the total sulfoxide is reduced by the reduction, alkylation, and trypsin cleavage necessary for our mass spectrometric analysis. Thus, our treatment results in a measurable but negligible (~0.1%) reduction of the sulfoxide.

Next we wanted to see how the ratio of MetSO213 to Met213 varied over the course of a prion disease. Forty hamsters were inoculated (*ic*) with 50 μL of a 1% brain homogenate. Each week, four animals were euthanized and their brains removed. Using the method of Diringer et al. (*37*), PrP 27−30 was isolated from each of the hamster brains. The quantity of MetSO213 and Met213 present in PrP 27−30 isolated from each brain was determined by mass spectrometric analysis using the internal standard. The data from this mass spectrometric analysis for weeks 3−10 were plotted as the ratio of MetSO213 to Met213 versus time as shown in Figure 4. For weeks 1 and 2, the signal for MetSO213 was not greater than noise, so these data sets were not included in the graph. The quantity of both Met213 and MetSO213 increased as the amount of PrP 27−30 increased over time (*31*). However, the ratio between the two remains nearly constant, which indicates that the increase in the amount of MetSO213 is proportional to the increase in the amount of Met213. Furthermore, as the quantity of PrP 27−30 increases

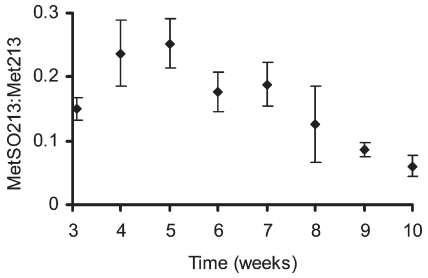

FIGURE 4: Ratios of the oxidized peptide to the unoxidized peptide isolated from the brains of hamsters during the course of an *ic* challenge with the 263K strain of hamster-adapted scrapie. Results are shown as means ± the standard deviation of data for PrP 27−30 (PK-treated protein) isolated from the brains of four animals per time point.

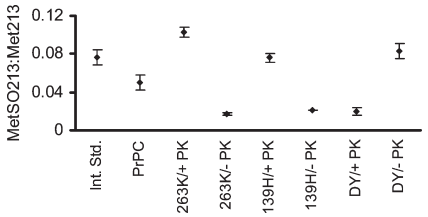

FIGURE 5: Comparison of the ratio of the oxidized peptide to the unoxidized peptide for the isotopically labeled internal standard, normal cellular prion protein (PrP^C), and three hamster-adapted prion strains (with or without PK).

from week 5 to 10, the proportion of MetSO213 actually decreases. The opposite would be expected if MetSO213-containing PrP^C were selectively converted to PrP^{Sc}. Instead, this is what would be expected if the oxidation were the result of the exposure to the low levels of oxidants present in normal laboratory solutions.

We wanted to see if other hamster-adapted prion strains with longer incubation periods behaved the same way as the 263K strain of hamster-adapted scrapie does. The 263K strain of hamster-adapted scrapie has a relatively short incubation period of 82 ± 1 days when inoculated *ic*. The 139H (175 ± 6 days) and drowsy (166 ± 10 days) strains have even longer incubation periods. A single brain from a symptomatic animal infected with the 139H, drowsy, or 263K strain was removed from a euthanized animal. The prions from each brain were isolated by the method of Diringer et al. (*37*). Each isolate was divided in two. Half was digested with proteinase K (PK+) to yield PrP 27−30. The other half (PK−) was not digested. Amounts of Met213 and MetSO213 were determined by mass spectrometry, and from this, the ratio of MetSO213 to Met213 was determined for each of these samples. The results for hamster-adapted prion strains 263K, 139H, and drowsy with PK treatment (0.1 ± 0.005, 0.08 ± 0.004, and 0.02 ± 0.004, respectively) and without PK treatment (0.02 ± 0.001, 0.02 ± 0.0006, and 0.08 ± 0.008, respectively) are shown in Figure 5. The ratio of MetSO213 to Met213 remains low regardless of the length of the incubation of the strain or whether it is treated with proteinase K.

The method we used to isolate PrP^{Sc} is based on the sedimentation characteristics of prion particles (*41*). Several ultracentrifugation-based isolation methods have been developed for the isolation of large amounts of PrP^{Sc} and adapted to small-scale isolation. All of these methods typically give a >90% yield of prions (based on a bioassay) in a given sample (*42*, *43*). The method we employ is a simpler version of these procedures that is

known to give purer preparations, but with lower yields of prions (*37*).

We were concerned that this simplified procedure might introduce a bias into the isolation procedure. We homogenized a single brain and took six aliquots. Three were subjected to the prion isolation procedure described by Diringer et al. (*37*). The other three were subjected to the prion isolation procedure of Bolton et al. that was reported to yield >90% of the prions present in the sample, based on a bioassay (*42*). These samples were quantitated by mass spectrometry. More PrP 27−30 was isolated by the method of Bolton et al. ($6 \times 10^2 \pm 1 \times 10^2$ pmol) than by the method of Diringer et al. ($3 \times 10^2 \pm 1 \times 10^2$ pmol). We calculated the ratio of MetSO213 to Met213 for both of these procedures. The method of Bolton et al. yielded a ratio of 0.05 ± 0.003, and the method of Diringer et al. yielded a ratio of 0.06 ± 0.005. There is no statistical difference between these ratios ($p > 0.01$), which indicates that no bias occurs during the isolation of PrP^{Sc}.

We used the internal standard to estimate the amount of oxidation that occurs in preparing and handling a sample for mass spectrometry. The isotopically labeled internal standard peptide was purified and analyzed by the vendor. We selected an aliquot of this purified internal standard that had undergone several freeze−thaw cycles and had been exposed to atmospheric oxygen. It was added to the redissolved pellet before reduction, alkylation, and trypsin cleavage. Thus, the ratio of MetSO to Met present in the internal standard would provide us with an estimate of the oxidation that occurs during sample processing and analysis by mass spectrometry. The MRM method was amended to include transitions for the sulfoxide of the isotopically labeled internal standard. Four samples were run, and the area ratios were calculated for each compound. The ratio was determined to be 0.08 ± 0.008, indicating that approximately 8% of the methionine in the internal standard is oxidized as a result of the process of sample handling and mass spectrometric analysis. This level of oxidation is comparable to that observed in other in-solution digestions (*44*). A comparison of this value with that obtained from the analysis of other strains of hamster-adapted PrP^{Sc} (with or without PK) and PrP^{C} is shown in Figure 5.

Lastly, we isolated PrP^{C} from the brains of healthy uninfected animals for comparison with the prions (with or without PK) isolated from the brains of infected animals. These animals were obtained from a commercial vendor and had never been housed in an area exposed to prions. The source material was from a mixture of 300 hamsters, so it should give a broad average measure of the MetSO213 to Met213 ratio present in a healthy uninfected hamster. The PrP^{C} was purified by cation exchange chromatography and immobilized metal affinity chromatography (IMAC) of the solubilized synaptosomal/microsomal membranes (*39*). The purification was followed by Western blotting using the 3F4 antibody. The estimated yield of the purified PrP^{C} protein was <10% of the total PrP^{C} present in the brain (*39*). The results from the mass spectrometric quantitation are shown in Figure 5. PrP^{C} has a low ratio of MetSO213 to Met213, which is not surprising since it has a high rate of turnover relative to that of a prion (*45*). It is surprising that the ratio is similar to that of the PrP^{Sc} isolated from the brains of infected hamsters.

Other researchers have reported that the addition 5 mM $CuCl_2$ during the refolding of recombinant mouse PrP results in the oxidation of 70−80% of the total methionine present in the protein (*17*). If the same amount of $CuCl_2$ is added to renatured recombinant mouse PrP, then less than 10% of the total methionine present in the protein is oxidized (*17*). The PrP^{C} isolation procedure we use does not involve refolding of the molecule, but it does employ copper(II) as the metal in the immobilized metal affinity chromatography step of the isolation procedure; therefore, we were concerned that the immobilized copper might oxidize the Met213 in hamster PrP^{C}. We renatured recombinant hamster PrP using copper-immobilized metal affinity chromatography (*46*) and determined the ratio of MetSO213 to Met213 present in our recombinant hamster PrP to be 0.02 ± 0.005. From this, we conclude that the immobilized copper(II), unlike free copper(II), does not result in significant oxidation of the chromatographed protein.

DISCUSSION

Our mass spectrometry-based method uses chromatographic retention times and MRM to identify and quantify an analyte peptide. This allows us to directly detect and quantitate the tryptic digest peptide containing Met213. We used this method to show that the ratio of MetSO213 to Met213 is low in both PrP^{C} and PrP^{Sc}. Furthermore, this ratio is comparable to that observed by the handling necessary to perform our mass spectrometric analysis. During a time course, the ratio of MetSO213 to Met213 remains low, and as the disease progresses, the ratio decreases. It remains low in symptomatic animals infected with prion strains (139H and drowsy) with incubation times much longer than that of 263K. These results support the hypothesis that MetSO213 should not be regarded as a prion-specific covalent signature in hamsters.

Our work is done in solution and under conditions where the generation of reactive oxygen species is minimized (*26*). In the past, we used SDS−PAGE to purify the prions before quantitation (*30*). We detected the presence of the oxidized form of cysteine, cysteic acid, in samples of PrP 27−30 run on SDS−PAGE gels. Upon closer examination, we realized that cysteic acid was produced when a sample was run on an SDS−PAGE gel without the addition DTT or β-mercaptoethanol (data not shown). In retrospect, we should not have been surprised that oxidation should occur during gel electrophoresis (*24*−*27*). It is not remarkable that oxidation of methionine could occur under such conditions (*26*). Since then, we have opted for a solution-based method of analysis and have not observed the presence of cysteic acid.

Our data do not exclude the possibility that there is an enzyme or enzymes that specifically reduce MetSO213 to Met213. Such enzymes (methionine sulfoxide reducing enzymes, MsrA and MsrB) are known to exist and are actively involved in reducing MetSO to Met on the basis of the stereochemistry of the sulfoxide (*47*). These enzymes are found in a variety of organisms (*48*). They are most active on methionines found on the surfaces of proteins. Since Met213 is part of α-helix 3, adjacent to the disulfide bond, and is relatively resistant to oxidation by hydrogen peroxide (*18*), it is not likely to be found on the surface of the protein and subjected to ready reduction. α-Helix 3 is not degraded by partial proteinase K digestion, which suggests that Met213 remains relatively inaccessible from the surface. It is therefore unlikely that an Msr is responsible for the small amounts of MetSO213 found in our samples.

Since we inoculated our animals with the 263K strain of hamster-adapted scrapie, our data have no bearing on the origin of spontaneous prion diseases. It does not exclude or support the possibility that oxidation of Met213 to MetSO213 could be a

primary event in the spontaneous formation of a prion (*20*, *21*). Once formed, the prion would then recruit and convert PrP^{C} into PrP^{Sc}. Since a single ID_{50} is estimated to contain fewer than 1 million molecules (*49*, *50*), the most infectious prion particles contain fewer than 30 molecules (*51*), and the minimum size for a prion is estimated to be three molecules (*52*, *53*), our method would not be sufficiently sensitive to detect this proposed seed (*30*). In any event, the original seed would most likely be lost during the natural turnover of prions (*45*).

Our data do allow us to conclude that, in hamsters, it is unlikely that MetSO213 is a covalent prion signature. It does not appear that PrP^{C} possessing MetSO213 is selectively recruited and then converted to PrP^{Sc}. The observed MetSO213 is most likely the result of oxidation that can occur in proteins with relatively low turnover rates or when femtomole amounts of proteins are handled in the presence of atmospheric oxygen.

REFERENCES

1. Prusiner, S. B. (1982) Novel proteinaceous infectious particles cause scrapie. *Science 216*, 136–144.
2. Prusiner, S. B. (1998) Prions. *Proc. Natl. Acad. Sci. U.S.A. 95*, 13363–13383.
3. Detwiler, L. A., and Baylis, M. (2003) The epidemiology of scrapie. *Rev. Sci. Tech. 22*, 121–143.
4. Harman, J. L., and Silva, C. J. (2009) Bovine spongiform encephalopathy. *J. Am. Vet. Med. Assoc. 234*, 59–72.
5. Kirkwood, J. K., and Cunningham, A. A. (1994) Epidemiological observations on spongiform encephalopathies in captive wild animals in the British Isles. *Vet. Rec. 135*, 296–303.
6. Marsh, R. F., and Hadlow, W. J. (1992) Transmissible mink encephalopathy. *Rev. Sci. Tech. 11*, 539–550.
7. Williams, E. S. (2005) Chronic wasting disease. *Vet. Pathol. 42*, 530–549.
8. Stahl, N., Baldwin, M., Teplow, D. B., Hood, L. E., Beavis, R., Chait, B., Gibson, B. W., Burlingame, A. L., and Prusiner, S. B. (1992) Cataloging post-translational modifications of the scrapie prion protein by mass spectrometry. In Prion diseases of humans and animals (Prusiner, S. B., Collinge, J., Powell, J., and Anderton, B., Eds.) pp 361−379, Ellis Horwood, New York.
9. Stahl, N., Baldwin, M. A., Teplow, D. B., Hood, L., Gibson, B. W., Burlingame, A. L., and Prusiner, S. B. (1993) Structural studies of the scrapie prion protein using mass spectrometry and amino acid sequencing. *Biochemistry 32*, 1991–2002.
10. Rudd, P. M., Endo, T., Colominas, C., Groth, D., Wheeler, S. F., Harvey, D. J., Wormald, M. R., Serban, H., Prusiner, S. B., Kobata, A., and Dwek, R. A. (1999) Glycosylation differences between the normal and pathogenic prion protein isoforms. *Proc. Natl. Acad. Sci. U.S.A. 96*, 13044–13049.
11. Stimson, E., Hope, J., Chong, A., and Burlingame, A. L. (1999) Site-specific characterization of the N-linked glycans of murine prion protein by high-performance liquid chromatography/electrospray mass spectrometry and exoglycosidase digestions. *Biochemistry 38*, 4885–4895.
12. Stahl, N., Baldwin, M. A., Hecker, R., Pan, K. M., Burlingame, A. L., and Prusiner, S. B. (1992) Glycosylinositol phospholipid anchors of the scrapie and cellular prion proteins contain sialic acid. *Biochemistry 31*, 5043–5053.
13. Caughey, B. W., Dong, A., Bhat, K. S., Ernst, D., Hayes, S. F., and Caughey, W. S. (1991) Secondary structure analysis of the scrapie-associated protein PrP 27−30 in water by infrared spectroscopy. *Biochemistry 30*, 7672–7680.
14. Safar, J., Roller, P. P., Gajdusek, D. C., and Gibbs, C. J., Jr. (1993) Conformational transitions, dissociation, and unfolding of scrapie amyloid (prion) protein. *J. Biol. Chem. 268*, 20276–20284.
15. Riek, R., Hornemann, S., Wider, G., Billeter, M., Glockshuber, R., and Wuthrich, K. (1996) NMR structure of the mouse prion protein domain PrP(121−321). *Nature 382*, 180–182.
16. James, T. L., Liu, H., Ulyanov, N. B., Farr-Jones, S., Zhang, H., Donne, D. G., Kaneko, K., Groth, D., Mehlhorn, I., Prusiner, S. B., and Cohen, F. E. (1997) Solution structure of a 142-residue recombinant prion protein corresponding to the infectious fragment of the scrapie isoform. *Proc. Natl. Acad. Sci. U.S.A. 94*, 10086–10091.
17. Wong, B. S., Wang, H., Brown, D. R., and Jones, I. M. (1999) Selective oxidation of methionine residues in prion proteins. *Biochem. Biophys. Res. Commun. 259*, 352–355.
18. Requena, J. R., Dimitrova, M. N., Legname, G., Teijeira, S., Prusiner, S. B., and Levine, R. L. (2004) Oxidation of methionine residues in the prion protein by hydrogen peroxide. *Arch. Biochem. Biophys. 432*, 188–195.
19. Breydo, L., Bocharova, O. V., Makarava, N., Salnikov, V. V., Anderson, M., and Baskakov, I. V. (2005) Methionine oxidation interferes with conversion of the prion protein into the fibrillar proteinase K-resistant conformation. *Biochemistry 44*, 15534–15543.
20. Colombo, G., Meli, M., Morra, G., Gabizon, R., and Gasset, M. (2009) Methionine sulfoxides on prion protein helix-3 switch on the α-fold destabilization required for conversion. *PLoS One 4*, e4296.
21. Wolschner, C., Giese, A., Kretzschmar, H. A., Huber, R., Moroder, L., and Budisa, N. (2009) Design of anti- and pro-aggregation variants to assess the effects of methionine oxidation in human prion protein. *Proc. Natl. Acad. Sci. U.S.A. 106*, 7756–7761.
22. Canello, T., Engelstein, R., Moshel, O., Xanthopoulos, K., Juanes, M. E., Langeveld, J., Sklaviadis, T., Gasset, M., and Gabizon, R. (2008) Methionine sulfoxides on PrPSc: A prion-specific covalent signature. *Biochemistry 47*, 8866–8873.
23. Kotiaho, T., Eberlin, M. N., Vainiotalo, P., and Kostiainen, R. (2000) Electrospray mass and tandem mass spectrometry identification of ozone oxidation products of amino acids and small peptides. *J. Am. Soc. Mass Spectrom. 11*, 526–535.
24. Guan, Z., Yates, N. A., and Bakhtiar, R. (2003) Detection and characterization of methionine oxidation in peptides by collision-induced dissociation and electron capture dissociation. *J. Am. Soc. Mass Spectrom. 14*, 605–613.
25. Chowdhury, S. K., Eshraghi, J., Wolfe, H., Forde, D., Hlavac, A. G., and Johnston, D. (1995) Mass spectrometric identification of amino acid transformations during oxidation of peptides and proteins: Modifications of methionine and tyrosine. *Anal. Chem. 67*, 390–398.
26. Sun, G., and Anderson, V. E. (2004) Prevention of artifactual protein oxidation generated during sodium dodecyl sulfate-gel electrophoresis. *Electrophoresis 25*, 959–965.
27. Swiderek, K. M., Davis, M. T., and Lee, T. D. (1998) The identification of peptide modifications derived from gel-separated proteins using electrospray triple quadrupole and ion trap analyses. *Electrophoresis 19*, 989–997.
28. Chen, M., and Cook, K. D. (2007) Oxidation artifacts in the electrospray mass spectrometry of Aβ peptide. *Anal. Chem. 79*, 2031–2036.
29. Morand, K., Talbo, G., and Mann, M. (1993) Oxidation of peptides during electrospray ionization. *Rapid Commun. Mass Spectrom. 7*, 738–743.
30. Onisko, B., Dynin, I., Requena, J. R., Silva, C. J., Erickson, M., and Carter, J. M. (2007) Mass spectrometric detection of attomole amounts of the prion protein by nanoLC/MS/MS. *J. Am. Soc. Mass Spectrom. 18*, 1070–1079.
31. Onisko, B. C., Silva, C. J., Dynin, I., Erickson, M., Vensel, W. H., Hnasko, R., Requena, J. R., and Carter, J. M. (2007) Sensitive, preclinical detection of prions in brain by nanospray liquid chromatography/tandem mass spectrometry. *Rapid Commun. Mass Spectrom. 21*, 4023–4026.
32. Kimberlin, R. H., and Walker, C. (1977) Characteristics of a short incubation model of scrapie in the golden hamster. *J. Gen. Virol. 34*, 295–304.
33. Marsh, R. F., and Kimberlin, R. H. (1975) Comparison of scrapie and transmissible mink encephalopathy in hamsters. II. Clinical signs, pathology, and pathogenesis. *J. Infect. Dis. 131*, 104–110.
34. Bessen, R. A., and Marsh, R. F. (1992) Identification of two biologically distinct strains of transmissible mink encephalopathy in hamsters. *J. Gen. Virol. 73*, 329–334.
35. Kimberlin, R. H., Cole, S., and Walker, C. A. (1987) Temporary and permanent modifications to a single strain of mouse scrapie on transmission to rats and hamsters. *J. Gen. Virol. 68*, 1875–1881.
36. Race, R. E., and Raymond, G. J. (2004) Inactivation of transmissible spongiform encephalopathy (prion) agents by environ LpH. *J. Virol. 78*, 2164–2165.
37. Diringer, H., Beekes, M., Ozel, M., Simon, D., Queck, I., Cardone, F., Pocchiari, M., and Ironside, J. W. (1997) Highly infectious purified preparations of disease-specific amyloid of transmissible spongiform encephalopathies are not devoid of nucleic acids of viral size. *Intervirology 40*, 238–246.
38. Prusiner, S. B., Groth, D., Serban, A., Stahl, N., and Gabizon, R. (1993) Attempts to restore scrapie prion infectivity after exposure to protein denaturants. *Proc. Natl. Acad. Sci. U.S.A. 90*, 2793–2797.

39. Pergami, P., Jaffe, H., and Safar, J. (1996) Semipreparative chromatographic method to purify the normal cellular isoform of the prion protein in nondenatured form. *Anal. Biochem. 236*, 63–73.
40. Houghten, R. A., and Li, C. H. (1979) Reduction of sulfoxides in peptides and proteins. *Anal. Biochem. 98*, 36–46.
41. Prusiner, S. B., Hadlow, W. J., Eklund, C. M., and Race, R. E. (1977) Sedimentation properties of the scrapie agent. *Proc. Natl. Acad. Sci. U.S.A. 74*, 4656–4660.
42. Bolton, D. C., Rudelli, R. D., Currie, J. R., and Bendheim, P. E. (1991) Copurification of Sp33−37 and scrapie agent from hamster brain prior to detectable histopathology and clinical disease. *J. Gen. Virol. 72*, 2905–2913.
43. Prusiner, S. B., Bowman, K. A., and Groth, D. F. (1987) Purification of scrapie prions. In Prions: Novel infectious pathogens causing scrapie and Creutzfeldt-Joakb disease (Prusiner, S. B., and McKinley, M. P., Eds.) pp 149−171, Academic Press, San Diego.
44. Froelich, J. M., and Reid, G. E. (2008) The origin and control of ex vivo oxidative peptide modifications prior to mass spectrometry analysis. *Proteomics 8*, 1334–1345.
45. Safar, J. G., DeArmond, S. J., Kociuba, K., Deering, C., Didorenko, S., Bouzamondo-Bernstein, E., Prusiner, S. B., and Tremblay, P. (2005) Prion clearance in bigenic mice. *J. Gen. Virol. 86*, 2913–2923.
46. Atarashi, R., Wilham, J. M., Christensen, L., Hughson, A. G., Moore, R. A., Johnson, L. M., Onwubiko, H. A., Priola, S. A., and Caughey, B. (2008) Simplified ultrasensitive prion detection by recombinant PrP conversion with shaking. *Nat. Methods 5*, 211–212.
47. Boschi-Muller, S., Gand, A., and Branlant, G. (2008) The methionine sulfoxide reductases: Catalysis and substrate specificities. *Arch. Biochem. Biophys. 474*, 266–273.
48. Weissbach, H., Resnick, L., and Brot, N. (2005) Methionine sulfoxide reductases: History and cellular role in protecting against oxidative damage. *Biochim. Biophys. Acta 1703*, 203–212.
49. Prusiner, S. B., Bolton, D. C., Groth, D. F., Bowman, K. A., Cochran, S. P., and McKinley, M. P. (1982) Further purification and characterization of scrapie prions. *Biochemistry 21*, 6942–6950.
50. Prusiner, S. B., McKinley, M. P., Bowman, K. A., Bolton, D. C., Bendheim, P. E., Groth, D. F., and Glenner, G. G. (1983) Scrapie prions aggregate to form amyloid-like birefringent rods. *Cell 35*, 349–358.
51. Silveira, J. R., Raymond, G. J., Hughson, A. G., Race, R. E., Sim, V. L., Hayes, S. F., and Caughey, B. (2005) The most infectious prion protein particles. *Nature 437*, 257–261.
52. Alper, T., Haig, D. A., and Clarke, M. C. (1966) The exceptionally small size of the scrapie agent. *Biochem. Biophys. Res. Commun. 22*, 278–284.
53. Bellinger-Kawahara, C. G., Kempner, E., Groth, D., Gabizon, R., and Prusiner, S. B. (1988) Scrapie prion liposomes and rods exhibit target sizes of 55,000 Da. *Virology 164*, 537–541.